CEA/DAPNIA/SEA-97-14

Luminosity Monitor Studies for TESLA

Olivier NAPOLY
CEA, DSM/DAPNIA
CE-Saclay, F-91191 Gif-sur-Yvette Cedex, France

and

Daniel SCHULTE
CERN, PS/LP
CH-1211 Genève 23, Suisse

November 10, 1997

Abstract

The feasibility of a luminosity monitor based on a radiative Bhabha detector is investigated in the context of the TESLA linear collider. Another option based on low energy e^+e^- pair calorimetry is also discussed. In order to monitor the beam parameters at the interaction point by optimizing the luminosity, these detectors should be able to provide a relative measurement of the luminosity with a resolution better than 1% using only a fraction of the TESLA bunch train.

1 Introduction

The optical tuning of the transverse beam sizes at the interaction point (IP) of an e^+e^- linear collider will be part of the machine start-up procedures. For TESLA [1], given the beam parameters presented in Table 1, it is possible to measure the individual horizontal beam sizes with a Laser wire and the vertical ones with a Laser interferometer.

During the normal operation of the machine, while the beam are in collisions, the detuning of the final focus optics must be controlled in such a way that the luminosity stays maximum. The required on-line tuning procedure should be the least invasive in order to lose the least luminosity up-time. The beam-beam deflection scan method in use at the SLC [2] allows one to measure the convoluted spot sizes of both beams with a limited impact on the machine operation. For TESLA however, the large vertical disruption of the colliding beams, characterised by the disruption parameter $D_y = 18$, precludes the measurement of the vertical spot size by this method. However, the combination of beam-beam horizontal deflection scans ($D_x = 0.4$) and of luminosity monitoring would be a valid procedure to correct both horizontal and vertical aberrations. A relative measurement of the luminosity should be sufficient for that purpose.

Beam sizes	σ_x^*, σ_y^*	[nm]	845 , 19
Emittances	$\gamma\epsilon_x^*, \gamma\epsilon_y^*$	[μm]	14 , 0.25
Bunch length	σ_z	[mm]	0.7
Bunch population	N_e	[10^{10}]	3.63
Number of bunch per train	n_b		1130
Bunch spacing	Δt_b	[ns]	708
Luminosity	$\mathcal{L}$	[10^{33} cm^{-2}s^{-1}]	6
Beamstrahlung	δ_B	[%]	2.5
Divergences	θ_x^*, θ_y^*	[μrad]	34 , 27
Beta	β_x^*, β_y^*	[mm]	25 , 0.7

Table 1: TESLA beam parameters at the IP for $\sqrt{s} = 500$ GeV

Bhabha monitors are a well proven instruments for luminosity measurement at e^+e^- and e^-p colliders [3]. For TESLA as well as for any future linear colliders, such a monitor should integrate the 3 following constraints:

1. the need for high rates to provide on-line monitoring,

2. the beamstrahlung photon background around the beam axis,

3. the sensitivity of the Bhabha rates and angular distributions to finite beam size and beam-beam effects.

The first constraint, common to all colliders, leads to adopt the radiative Bhabha process $e^+e^- \to e^+e^-\gamma$, also called bremsstrahlung, where one of the leptons loses energy by emitting a high energy photon. This process has a much higher event rate at small angles than the elastic Bhabha process $e^+e^- \to e^+e^-$. The second constraint, already met at the SLC, is solved by detecting the low-energy electron deflected away from the beamstrahlung cone by the focusing lens close to the IP, rather than detecting the photons at low angles.

The finite beam size effect [4], although already present at VEPP2, LEP or SLC, is more critical for the future linear colliders with the very small spot sizes and the high disruption beam-beam effects. Indeed, not only the bremsstrahlung cross-section must be weighted by the luminosity which varies during the collision, but the outgoing low energy leptons are strongly deflected by the opposite beam, resulting in a large smearing of their angular distribution. For example, in the case of TESLA, the beam-beam effect increases the horizontal angular spread of the bremsstrahlung particles with energies from 10 GeV to 90 GeV from about 45 μrad up to 660 μrad. This widening of the angular spread enhances the rate of low energy leptons deflected at angles usable for a luminosity detector. This more than counterbalances the finite beam size correction of roughly 1/2 in the bremsstrahlung rate.

Because of its sensitivity to the beam-beam effect, the bremsstrahlung signal within a fixed kinematical acceptance is no longer proportional to the luminosity. Consider for instance the case where a smaller horizontal spot size combined with a larger vertical one at constant luminosity but higher vertical disruption ($D_y \propto (\sigma_x)^{-1}\,(\sigma_y^*)^0$), would nevertheless lead to a larger bremsstrahlung rate due to stronger beam-beam forces and a larger smearing of the bremsstrahlung energy and angular distributions. However this signal can still be used for measuring luminosity variations induced by beam parameter changes at the IP such that the horizontal spot sizes and horizontal divergences of both beams are unchanged. This includes the most important vertical aberrations. As mentioned above, the combination of horizontal beam-beam deflection scans for measuring the horizontal aberrations and of luminosity scans for the vertical ones provides therefore a complete tuning strategy. This strategy, recently re-investigated at the SLC [7], offers the advantage that luminosity monitoring is less invasive than the vertical beam-beam deflection scans since the beam aberrations can be measured in the vicinity of the optimal head-on collision parameters.

The main purpose of this study is to characterize the expected bremsstrahlung signal in terms of energy spectrum and rate, and to calculate the achievable resolution for measuring the luminosity in a given integration time. The case of the vertical spot size tuning will be considered in details by computer simulations of the scans of linear matrix aberrations.

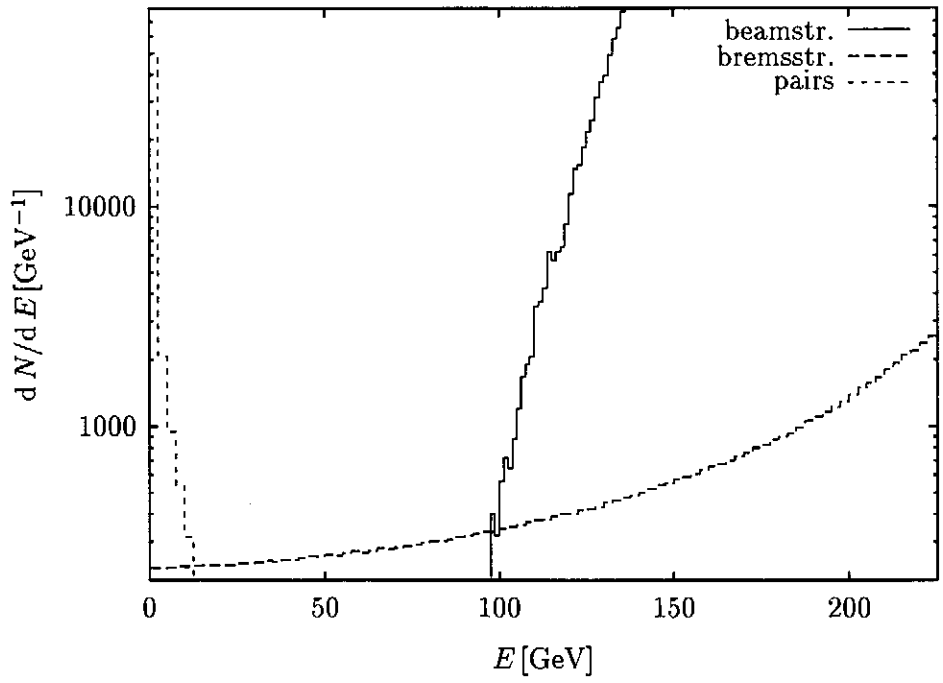

Figure 1: The energy spectrum of the particles due to pair production, bremsstrahlung and beamstrahlung for TESLA (500 GeV c.m.) parameters.

2 Bremsstrahlung Simulations of a Single Bunch Collision

As discussed in the introduction, the combination of finite beam size corrections to the bremsstrahlung process and of the beam-beam forces during the collision, requires the use of computer simulation to characterize the bremsstrahlung signal. The program GUINEA_PIG [5] is used for this study. It calculates the beam-beam forces and the beamstrahlung photon emission. Moreover the Monte-Carlo method used to generate the bremsstrahlung particles takes the finite beam size effect [4] into account. The trajectory of the low energy leptons is also tracked through the coherent e.m. field of the opposite beam. The bremsstrahlung cross-section can be artificially enhanced by a multiplicative factor n_b which allows one, with a single beam-beam simulation, to track the bremsstrahlung particles originating from n_b bunch collisions. This is useful to integrate the signal from several bunch-crossings, as done in the following section, assuming that the beam parameters are fixed and their fluctuations can be neglected, a valid assumption since the bunch population is about 6 orders of magnitude larger than the generated bremsstrahlung population.

This section deals with single bunch collision and therefore n_b is set to 1. The e^+

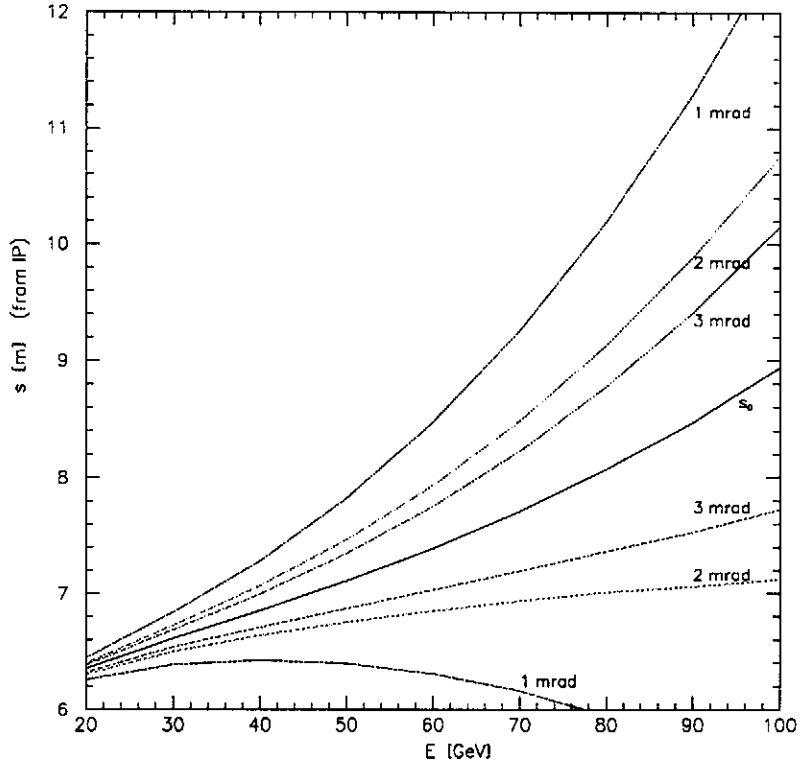

Figure 2: Background free region for a 24 mm the beam pipe radius

and e^- bunches are replaced by 40 000 macroparticles with 6-dimensional Gaussian distributions set by the beam parameters given in Table 1. The luminosity of the nominal parameters is about $6.0 \times 10^{33}\,\mathrm{cm}^{-2}\mathrm{s}^{-1}$ including a factor about 1.6 from the pinch effect. The statistical relative error on the luminosity is about $7.5 \cdot 10^{-5}$ from numerical origin. This is small enough to be able to identify, from the simulations, fluctuations of the order of 10^{-3} in the bremsstrahlung rates as physical statistical fluctuations.

The energy spectrum of the bremsstrahlung leptons is plotted in Fig.(1), in comparison with the tail of the energy spectrum of the beam particles and the one from e^+e^- pairs. Both the bremsstrahlung and the e^+e^- spectra are proportional to the luminosity while the beam spectrum merely scales with the bunch population. The use of the e^+e^- pairs, mostly stopped by the mask close to the IP, for the luminosity measurement is discussed in Section 4. The useful energy range of the bremsstrahlung leptons is therefore between about 10 and 90 GeV where they dominate the total spec-

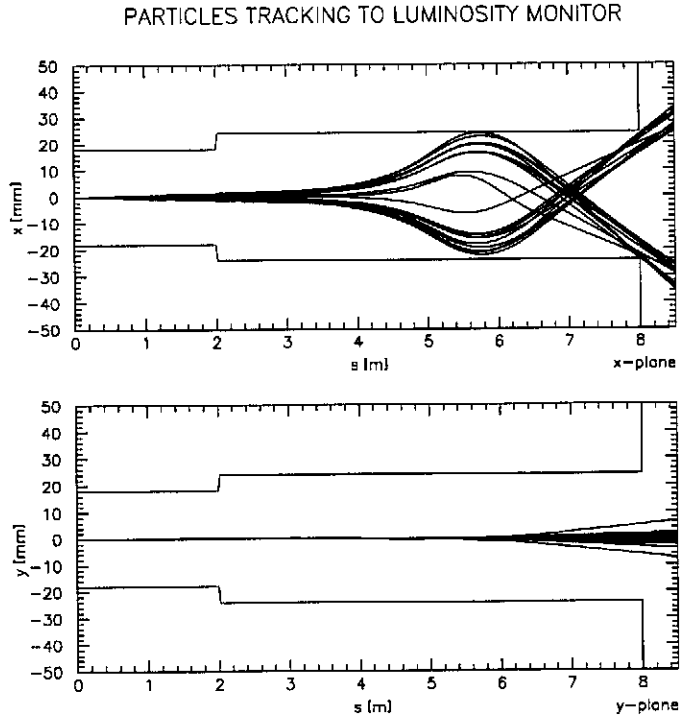

Figure 3: Trajectories from the IP hitting the luminosity monitor at 8.5 m

trum. This range corresponds to a region along the exit beam pipe, roughly between 7 m to 10 m from the IP, where the luminosity monitor can be located and be free from the background from the 90 GeV and higher energy spent beam particles. The reason is that the final doublet, designed for the 250 GeV beam, acts as a spectrometer by horizontally overfocusing these particles in such a way that the trajectory of the particles of a given energy E originating from the IP at any angle, crosses the beam axis at the location $s_0(E)$ where the so-called IP sine-like trajectory becomes zero. Therefore, there is a region around $s_0(E)$ where the particles with energy E cannot hit the beam pipe unless they have a very large horizontal angle with respect to the axis. Fig2 plots, for a beam pipe radius of 24 mm corresponding to the last doublet aperture, the region centered on the crossing abcissa $s_0(E)$ which is free from the background from particles of energy E with an angle at the IP less than 1 mrad, 2 mrad and 3 mrad. This plot shows that particles above 90 GeV and below 2 mrad IP angle, a safe upper limit according to beam-beam simulations, cannot hit the beam pipe between 7 m and 10 m. This is confirmed by simulations. It shows also that bremsstrahlung particles with 50 GeV energy cross the axis at about 7 m and can hit the beam pipe after 8 m even with IP angles below 1 mrad.

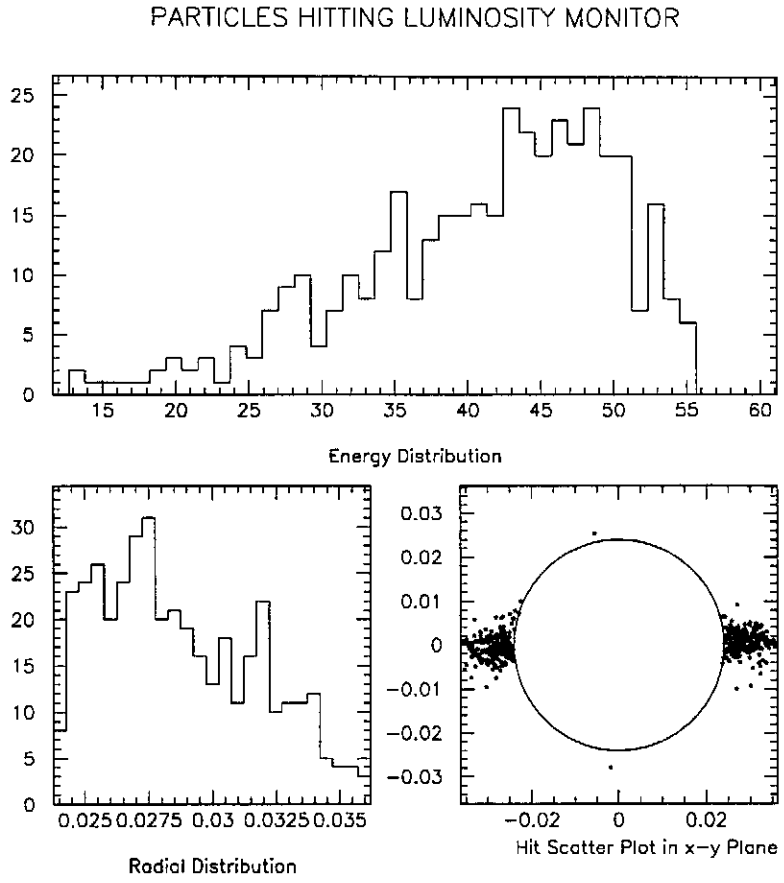

Figure 4: Energy and transverse distributions of the bremsstrahlung particles hitting the luminosity monitor for a single bunch crossing

For this study the luminosity monitor, assumed to be a hollow disk around the beam axis with 24 mm inner radius, is therefore located at 8.5 m from the IP. The traces of some bremsstrahlung particles impinging on the monitor are represented in Fig.(3) showing the strong horizontal overfocusing effect. The energy and transverse distributions of the bremsstrahlung leptons hitting the monitor from a single bunch crossing and with energies above 10 GeV, is shown in Fig.(4). Most hits are in the horizontal plane in such a way that the hollow disk could be replaced by vertical plates with the same aperture without losing more than 1% of signal. The small roll angle visible on the transverse scatter plot is due to the 3 T, 10 m long solenoid. As expected from the kinematical argument above, the monitor location is optimised for detecting about 50 GeV energy particles. The total number of hits is about 410 per side and per bunch crossing. Integrating over 25 bunch crossings should therefore lead to over

10000 total hits per side, enough to reduce the statistical error to the 1% level. This is confirmed by repeating 22 simulations with $n_b = 25$ using the same initial beam distributions: the relative dispersion in the number of hits is 8.5e-3. As can be seen from the energy distribution, the luminosity monitor location is optimised to detect 40 GeV to 50 GeV particles.

3 Vertical waist, vertical dispersion and coupling scans

The most important vertical beam parameters to be tuned are the beam matrix "rotations", also called "linear aberrations", which affect the vertical beam size, namely the vertical waist shift δw_y, the vertical dispersion η_y and the yx'-coupling c_y. The definition of these aberrations and the beam matrices associated to them are given in the Appendix. The beam matrices are used to generate the Gaussian distributions of the macro-particles entering the beam-beam and bremsstrahlung simulations.

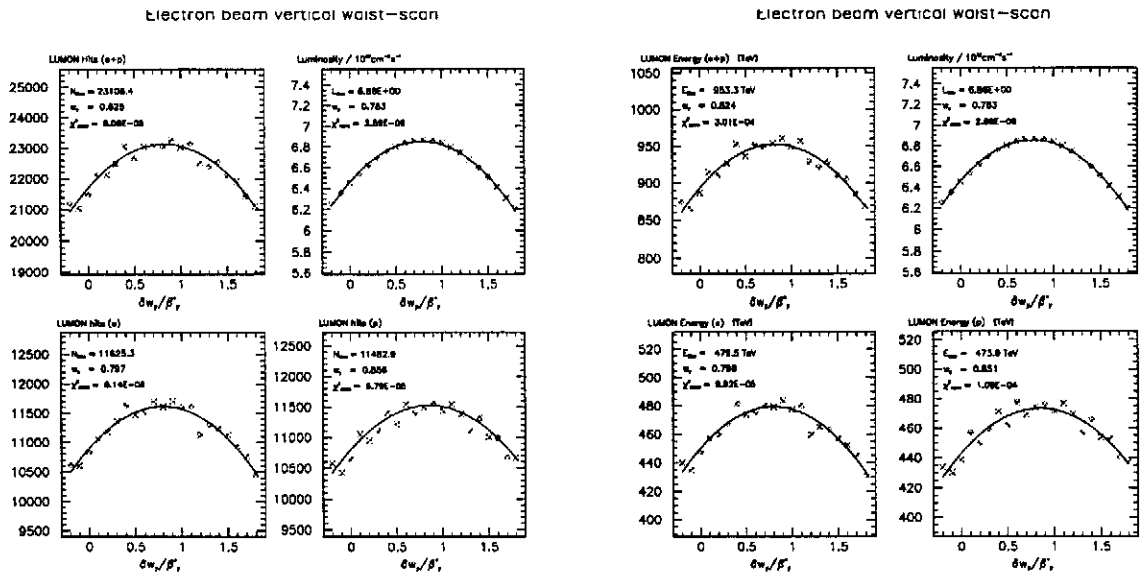

(a) (b)

Figure 5: Scan of the vertical waist shift: (a) numbers of hits (b) energy deposited on the luminosity detector. Parabolic fits are drawn through the data points

Figs.(5,6,7) display the results of luminosity optimisations obtained by varying the three linear aberrations δw_y, η_y and c_y of the electron beam matrix individually, keeping

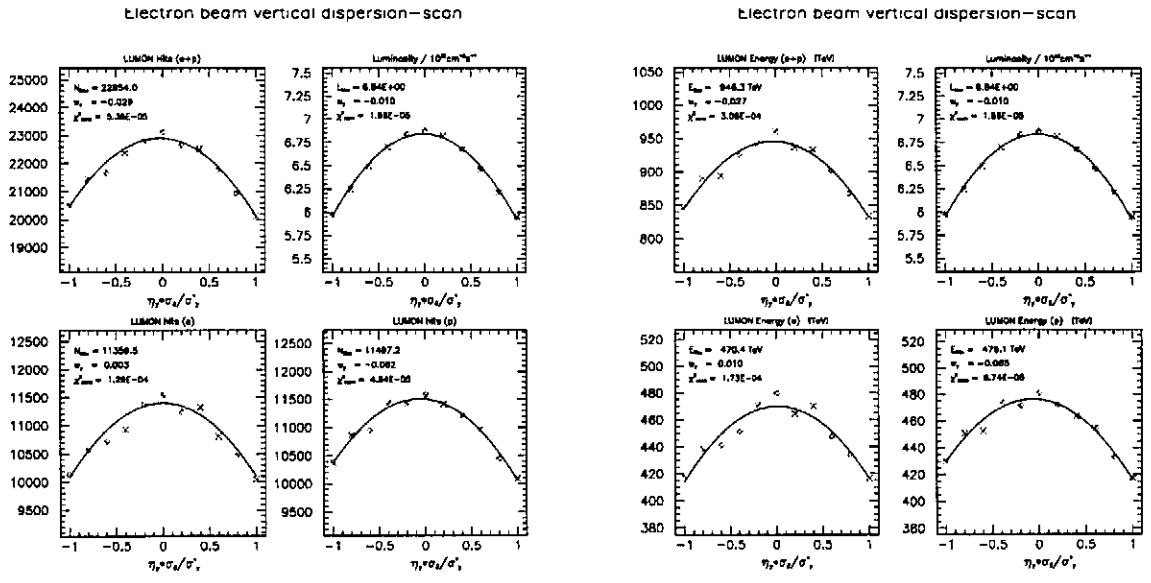

(a) (b)

Figure 6: Scan of the vertical dispersion: (a) numbers of hits (b) energy deposited on the luminosity detector. Parabolic fits are drawn through the data points

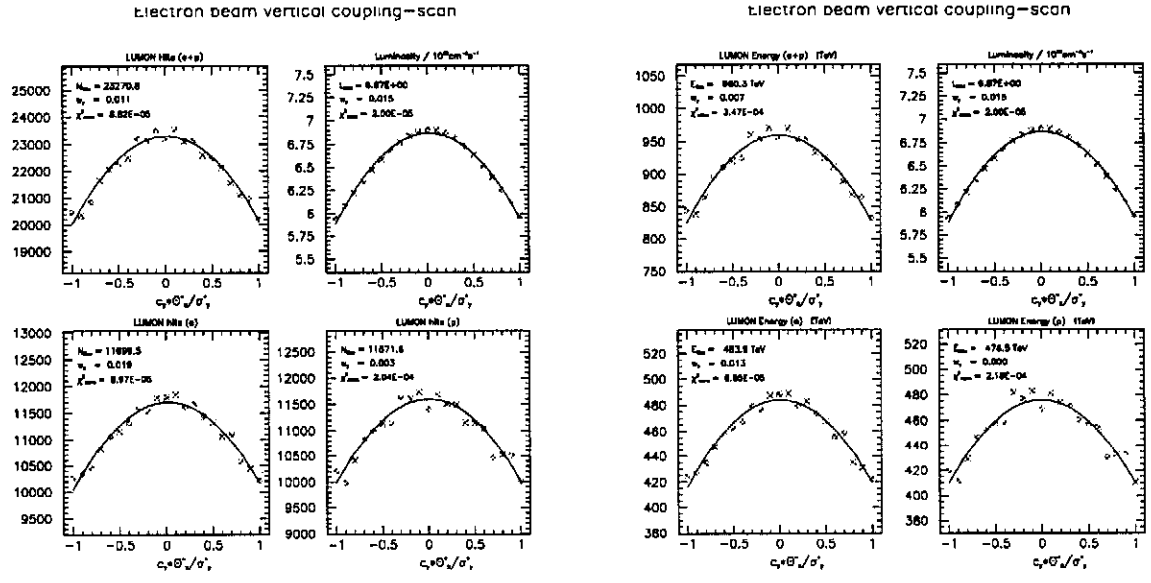

(a) (b)

Figure 7: Scan of the yx'-coupling: (a) numbers of hits (b) energy deposited on the luminosity detector. Parabolic fits are drawn through the data points

the positron beam constant. The central configuration is such that

$$\delta w_y^{(0)} = 0.8\,\beta_y^* \quad , \quad \eta_y^{(0)} = c_y^{(0)} = 0 \tag{1}$$

for both beams. It is also the optimal configuration since, due to the pinch effect, the luminosity is maximized when both beams have their vertical waist shifted by $0.8\,\beta_y^*$ in front of the IP. The gain in luminosity is about 14% with respect to the configuration where the waists are centered on the IP.

In the three figures, the part (a) plots the number of hits and the part (b) the energy deposited by bremsstrahlung particles on the luminosity monitor (on the electron side - lower left, on the positron side - lower right, and the sum of both sides - upper left). The calculated luminosity is shown in both upper right plots of parts (a) and (b). The parabolic fits $P(x)$ to the data points $(x_i, y_i)_{i=1,N}$ are superimposed and the position of the maxima is given in the plots together with the normalized chisquare defined as

$$\hat{\chi}^2 = \sum_{i=1}^{N} (y_i - P(x_i))^2 / \sum_{i=1}^{N} y_i^2 \tag{2}$$

The waist-shift and coupling scans in Figs.(5,7) involve 21 points, each of them integrating over 25 beam crossings, and therefore a total of 525 beam crossings. In order to test the influence of the number of data points on the fit precision, the dispersion scan involves only 11 points integrating 25 beam crossings and thus 275 beam crossings in total. The optimal luminosity as determined by parabolic fits can be compared with the maximum of the calculated luminosity. The relative precisions $\delta\mathcal{L}/\mathcal{L}$ obtained for the different scans are reported in Table 2. Clearly the luminosity optimum can be

	Waist	Dispersion	Coupling
e^--hits	$2.0 \cdot 10^{-5}$	$2.3 \cdot 10^{-5}$	$3.1 \cdot 10^{-6}$
e^+-hits	$5.1 \cdot 10^{-4}$	$3.6 \cdot 10^{-4}$	$1.7 \cdot 10^{-5}$
(e^-+e^+)-hits	$1.7 \cdot 10^{-4}$	$4.8 \cdot 10^{-5}$	$1.5 \cdot 10^{-6}$
e^--energy	$2.3 \cdot 10^{-5}$	$5.4 \cdot 10^{-5}$	$2.6 \cdot 10^{-7}$
e^+-energy	$4.5 \cdot 10^{-4}$	$4.0 \cdot 10^{-4}$	$2.8 \cdot 10^{-5}$
(e^-+e^+)-energy	$1.6 \cdot 10^{-4}$	$3.6 \cdot 10^{-5}$	$8.3 \cdot 10^{-6}$

Table 2: Relative precision $\delta\mathcal{L}/\mathcal{L}$ in the determination of the optimal luminosity for the various scans and signals from the luminosity monitor

determined equally from the number of hits on Bhabha counters, or from the energy deposited on calorimeters. The resolution should be better than 10^{-3} with about 500 bunch crossings for the waist scan, and about 250 crossings for the dispersion and coupling scans.

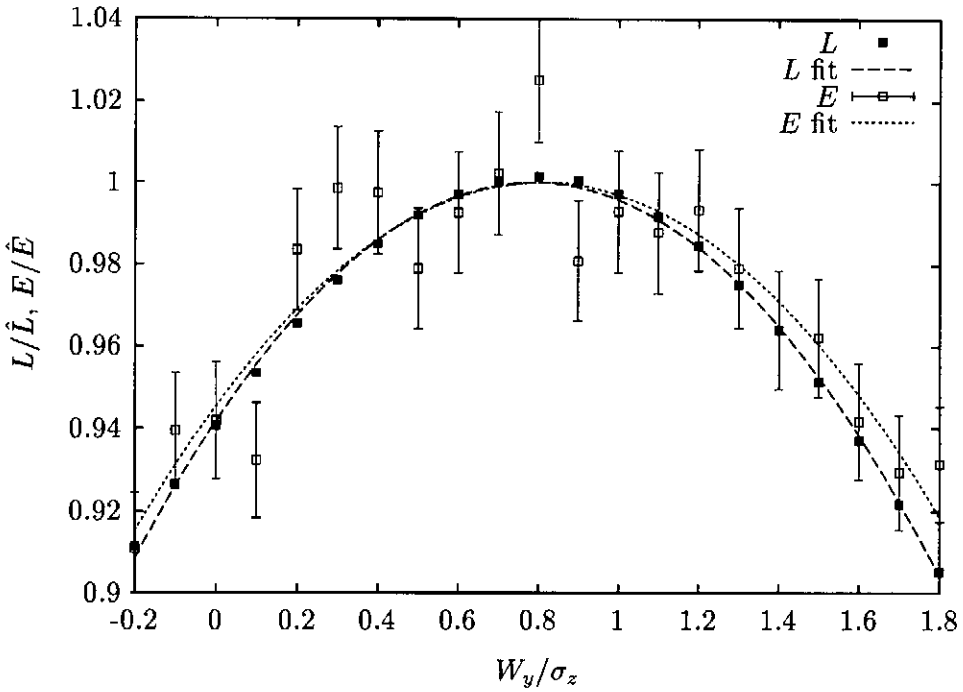

Figure 8: Scan of the vertical waist shift: energy deposited in the calorimeter and luminosity normalised to the maximal values.

In practice, each scan could be implemented by exciting a given closed orbit bump through the sextupole pairs of the chromatic correction section (CCS) [6] within one TESLA pulse [8]. A vertical waist scan, for instance, would be performed by exciting a symmetric closed bump through the vertical CCS sextupoles over 525 bunch crossings and measuring the luminosity for 525 monotonically increasing values of the waist-shift δw_y at the IP. The resolution achieved in such a scan should also be better than 10^{-3} since the statistical errors will be the same as for the scans presented above. In this way, a single TESLA bunch train with 1130 bunch crossings would allow one to measure the waist-shifts, or alternatively the dispersion and the coupling of both beams, provided the implementation of the necessary closed bumps is manageable within one pulse.

4 $e^+ - e^-$ Pair Calorimeter

Inside the main mask a combined inner mask and luminosity monitor will be installed. This inner mask will be hit by a large number of pairs deflected by the beams. At small radii it is covered with a low-Z material (graphite) to prevent the backscattering of low energy particles. At larger radii where the background due to the deflected pairs is small it will be used to measure the Bhabha events with larger angles. The rate of

these events will be a few per second, much higher than those measured in the main detector for the reconstruction of the luminosity spectrum but too low for monitoring.

The total energy deposited by the pairs in this mask can be measured calorimetrically, but details have to be worked out. This energy is about 9000 GeV per bunch crossing and per side. This values varies from simulation to simulation due to physical and numerical effects. Running 25 cases with the same initial distribution (read from a file) but different seeds for the random number generators showed an RMS-spread of 1.5 % and 2.0 % for the two sides. This is in reasonable agreement with the expectation from the counting rate alone (1.2 % from about 7700 hits). In practice one can expect significant contributions to the error from energy leaking out at the inner aperture of calorimeter and from jitter of the beam.

The scan was performed as for the former case. For each point only a single bunch crossing was measured. The optimal position of the waist was determined by maximising the sum of the two signals, leading to $\delta w_y = 0.81\,\beta_y^*$ (note that $\beta_y^* = \sigma_z$). The luminosity thus obtained is lower by a fraction of $5 \cdot 10^{-5}$ than the optimal value.

In contrast to the bremsstrahlung process where the production of particles depends strongly on the luminosity and only weakly on the other beam parameters, the number and energy of pairs produced depends also on the number and energy of the photons produced by beamstrahlung. The deflection is however very different in the two cases. The beam particles which have emitted bremsstrahlung are still relatively high in energy and are focused by the oncoming beam. Most of the particles from pair production that hit the calorimeter are low in energy and are defocused by the same charge oncoming beam. Combining the two methods one could thus hope for reducing possible ambiguities.

5 Conclusion

We believe that a luminosity monitor will be a necessary instrument for the fast tuning of the collision parameters of TESLA. In this study we have shown that a radiative Bhabha counter or calorimeter can monitor the luminosity to a 1% resolution by integrating the bremsstrahlung signal over about 25 TESLA bunch crossings, that is about 20 μs. In the suggested implementation, such a monitor should be optimised for lepton energies around 40 to 50 GeV with a rate of roughly 410 hits every 700 ns. A promising complementary option is a calorimeter in the masking system around the IP to measure the energy deposited by the pair-created e^+e^- particles. The 1% level can then be reached with one bunch crossing.

With either monitor, scanning the usual vertical linear aberrations with about 20 points should permit to determine the optimal luminosity to better than 0.1% relative resolution. Implementing such scans within a single TESLA bunch train should be possible: it would reduce considerably the influence of beam jitter on the luminosity

measurement errors.

Acknowledgements

We thank Stéphane Fartoukh and Andrei Sery for many useful discussions on the tracking and scanning algorithms.

A Beam matrix associated to vertical waist, vertical dispersion and yx'-coupling linear aberrations

Denoting by Σ_0^* the nominal beam matrix at the IP assumed diagonal in the usual set of TRANSPORT coordinates $(x, x', y, y', z, \delta)$,

$$\Sigma_0^* = \begin{pmatrix} \sigma_x^{*2} & 0 & 0 & 0 & 0 & 0 \\ 0 & \theta_x^{*2} & 0 & 0 & 0 & 0 \\ 0 & 0 & \sigma_y^{*2} & 0 & 0 & 0 \\ 0 & 0 & 0 & \theta_y^{*2} & 0 & 0 \\ 0 & 0 & 0 & 0 & \sigma_z^2 & 0 \\ 0 & 0 & 0 & 0 & 0 & \sigma_\delta^2 \end{pmatrix} \tag{3}$$

and, by R_0 and R the ideal and actual transfer matrices from an arbitrary point to the IP, the actual beam matrix at the IP, denoted by Σ^*, is then given by

$$\Sigma^* = (R \cdot R_0^{-1}) \cdot \Sigma_0^* \cdot (R \cdot R_0^{-1})^\top \tag{4}$$

The symplectic matrix $Q \stackrel{\text{def}}{=} R \cdot R_0^{-1}$ contains the most general linear aberrations generated by the optics upstream of the IP. Restricted to describe the vertical waist-shift q_{34}, the vertical dispersion q_{36} and the yx'-coupling q_{32}, this matrix can be parametrized as

$$Q = \begin{pmatrix} 1 & 0 & 0 & q_{32} & 0 & 0 \\ 0 & 1 & 0 & 0 & 0 & 0 \\ 0 & q_{32} & 1 & q_{34} & 0 & q_{36} \\ 0 & 0 & 0 & 1 & 0 & 0 \\ 0 & 0 & 0 & q_{36} & 1 & 0 \\ 0 & 0 & 0 & 0 & 0 & 1 \end{pmatrix} \tag{5}$$

The beam matrix at the IP is then given by

$$\Sigma^* = \begin{pmatrix} \sigma_x^{*2} + q_{32}^2\theta_y^{*2} & 0 & q_{32}q_{34}\theta_y^{*2} & q_{32}\theta_y^{*2} & q_{32}q_{36}\theta_y^{*2} & 0 \\ 0 & \theta_x^{*2} & q_{32}\theta_x^{*2} & 0 & 0 & 0 \\ q_{32}q_{34}\theta_y^{*2} & q_{32}\theta_x^{*2} & \sigma_y^{*2} + q_{32}^2\theta_x^{*2} + q_{34}^2\theta_y^{*2} + q_{36}^2\sigma_\delta^2 & q_{34}\theta_y^{*2} & q_{34}q_{36}\theta_y^{*2} & q_{36}\sigma_\delta^2 \\ q_{32}\theta_y^{*2} & 0 & q_{34}\theta_y^{*2} & \theta_y^{*2} & q_{36}\theta_y^{*2} & 0 \\ q_{32}q_{36}\theta_y^{*2} & 0 & q_{34}q_{36}\theta_y^{*2} & q_{36}\theta_y^{*2} & \sigma_z^2 + q_{36}^2\theta_y^{*2} & 0 \\ 0 & 0 & q_{36}\sigma_\delta^2 & 0 & 0 & \sigma_\delta^2 \end{pmatrix} \tag{6}$$

The shift of the longitudinal position of the vertical beam waist δw_y is given by the $\langle yy' \rangle$ correlation term and is therefore related to the q_{34} aberration by

$$\delta w_y = \langle yy' \rangle / \theta_y^{*2} = q_{34} \tag{7}$$

On the other hand, the vertical dispersion $\eta_y = q_{36}$ and the yx'-coupling term $c_y = q_{32}$ are related to the $\langle y\delta \rangle$ and $\langle yx' \rangle$ (or $\langle xy' \rangle$) correlations in the above beam matrix.

All three aberrations degrade the vertical spot size. The coupling term q_{32} degrades also the horizontal spot size but much less since, by considering its effect alone on the relative spot size growths, one gets

$$\frac{\delta\sigma_x^{*2}}{\sigma_x^{*2}} = \frac{\delta\sigma_y^{*2}}{\sigma_y^{*2}} \cdot \frac{\theta_y^{*2}}{\theta_x^{*2}} \cdot \frac{\sigma_y^{*2}}{\sigma_x^{*2}} \quad \ll \quad \frac{\delta\sigma_y^{*2}}{\sigma_y^{*2}} \tag{8}$$

since for the TESLA parameters (cf. Table 1), the horizontal and vertical beam divergences are roughly equal while the aspect ratio σ_x^*/σ_y^* is much larger than one.

Considering the effect of the three aberrations on the vertical spot size, it is convenient to introduce the normalized parameters

$$\begin{aligned} \hat{q}_{34} &= q_{34}\theta_y^*/\sigma_y^* \equiv \delta w_y/\beta_y^* \\ \hat{q}_{36} &= q_{36}\sigma_\delta/\sigma_y^* \equiv \eta_y\sigma_\delta/\sigma_y^* \\ \hat{q}_{32} &= q_{32}\theta_x^*/\sigma_y^* \equiv c_y\theta_x^*/\sigma_y^* \end{aligned} \tag{9}$$

in such a way that the relative spot-size growth reads

$$\frac{\delta\sigma_y^{*2}}{\sigma_y^{*2}} = \hat{q}_{32}^2 + \hat{q}_{34}^2 + \hat{q}_{36}^2 \tag{10}$$

These three normalized aberrations have been used in the scanning simulations discussed in the main text and they correspond to the scanning parameters along the horizontal axis of the plots shown in Figs.(5,6,7).

References

[1] "Conceptual Design of a 500 GeV e^+e^- Linear Collider with Integrated X-ray Laser Facility", R. Brinkmann, G. Materlick, J. Rossbach and A. Wagner Editors, DESY 1997-049 and ECFA 1997-182 (1997).

[2] P. Emma, L.J. Hendrickson, P. Raimondi and F. Zimmermann "Limitations of Interaction-Point Spot-Size Tuning at the SLC" SLAC-Pub-7509 (1997).

[3] V.N. Baier, V.S. Fadin, V.A. Khoze and E.A. Kuraev "Physics Reports 78, 3 (1981) 293-393.

[4] G.L. Kotkin, V.G. Serbo and A. Schiller "Process with Large Impact Parameters at Colliding Beams" Int. J. Mod. Phys. A, 4707 (1992).

[5] D. Schulte, "Study of Electromagnetic and Hadronic Background in the Interaction Region of TESLA", Ph.D. thesis, University of Hamburg 1996, and DESY report TESLA 97-08, April 1997

[6] N.J. Walker, J. Irwin and M. Woodley, "Global Tuning Knobs for the SLC Final Focus", SLAC-PUB-6207, Apr. 1993

[7] M. Ross Communication at the Linear Collider Workshop LC97, Zvenigorod Sept-Oct 1997

[8] The idea of using a single bunch train to perform a full luminosity scan was suggested to us by N.J. Walker.